Thermal Failure of a Nickel-base Superalloy Containing Carbonate Eutectic Salt

Madjid Sarvghad[1], Elaiza Luker[1], Stuart Bell[1], Ralf Raud[1], Theodore A. Steinberg[1] and Geoffrey Will[1]
[1]*Science and Engineering Faculty, Queensland University of Technology (QUT), Brisbane, Australia*
E-mail: madjid.sarvghadmoghaddam@hdr.qut.edu.au

Abstract

- An Inconel 601 crucible containing eutectic mixture of Li_2CO_3, K_2CO_3 and Na_2CO_3 was placed into a 450˚C preheated furnace.
- EBSD investigations confirmed the occurrence of partial recovery leading to stress relieving in the material.
- Failure was observed after 22 hours
- Cracking was of intergranular type resulted from:

I. Diffusion of oxygen and carbide forming elements through grain boundaries
II. High amount of residual stress
III. Microstructural evolution during thermal exposure

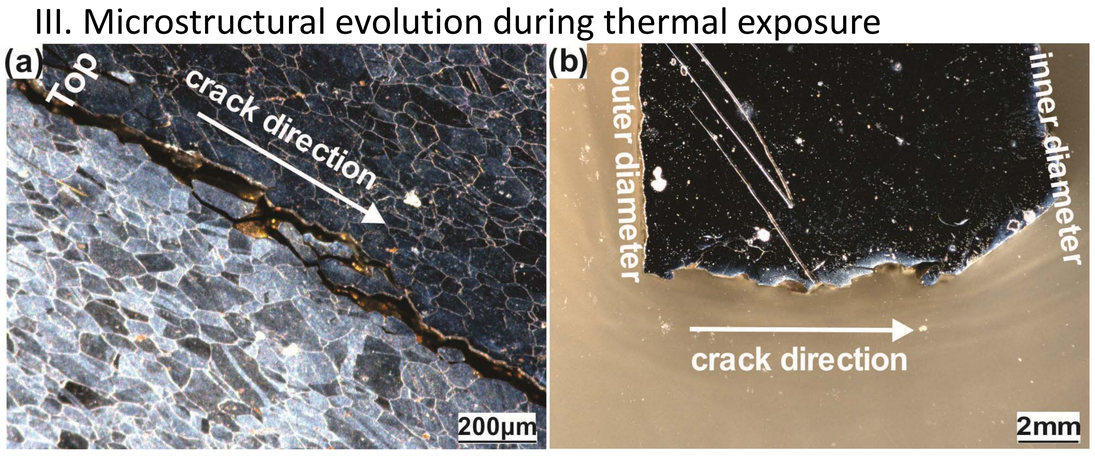

Figure 1. (a) Micro-graph image of the cracked crucible showing crack initiation area, top part of the crucible and growing direction downwards (etched sample), (b) top view macro-graph of the crucible sidewall showing outer and inner diameters and crack growth direction across the crucible wall (non-etched sample)

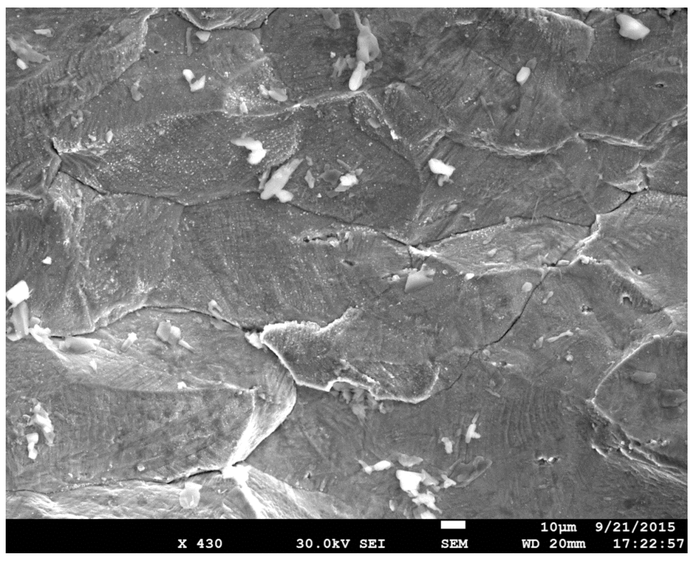

Figure 2. SEM-SE micrograph of the fracture surface showing grain boundary crack morphology and salt residue

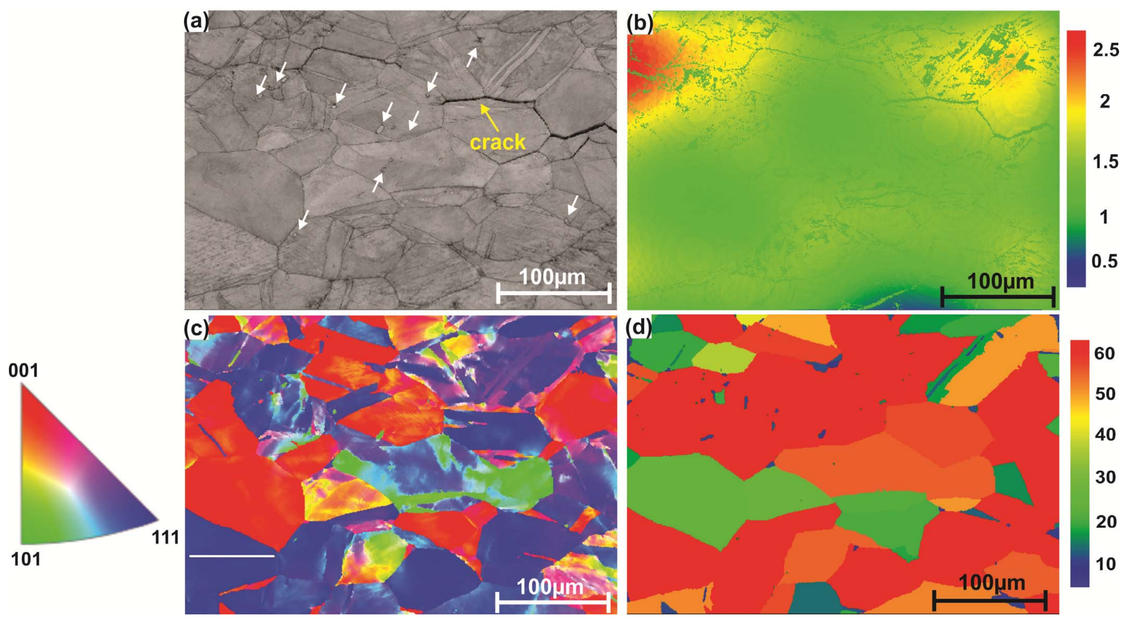

Figure 3. (a) Band contrast, (b) strain contouring map, (c) IPF X colour map, (d) maximum orientation spread map (MOS) of the same area in the cracked specimen (CS) including crack tip (yellow arrow). White arrows in (a) point to dispersed Ti-rich particles in the matrix; accelerating voltage= 25 kV, step size= 0.65 µm

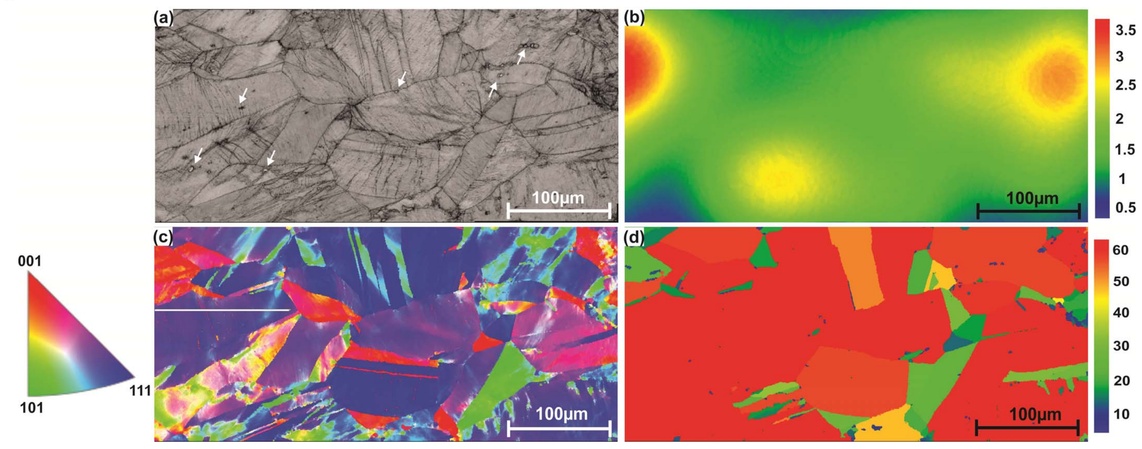

Figure 4. (a) Band contrast, (b) strain contouring map, (c) IPF X colour map, (d) maximum orientation spread map (MOS) of the same area in reference sample (RS). White arrows in (a) point to dispersed Ti-rich particles in the matrix; accelerating voltage= 30 kV, step size= 0.5 µm

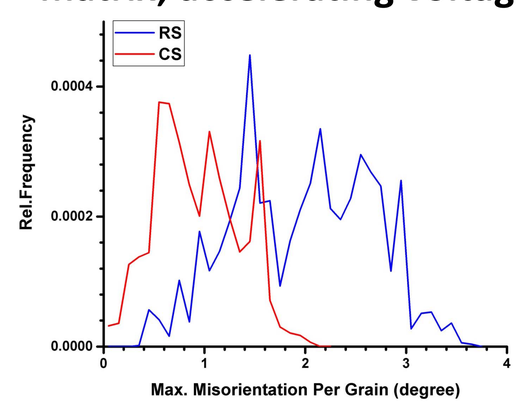

Figure 5. Strain contouring profile corresponding to maps in Figures.3b and 4b

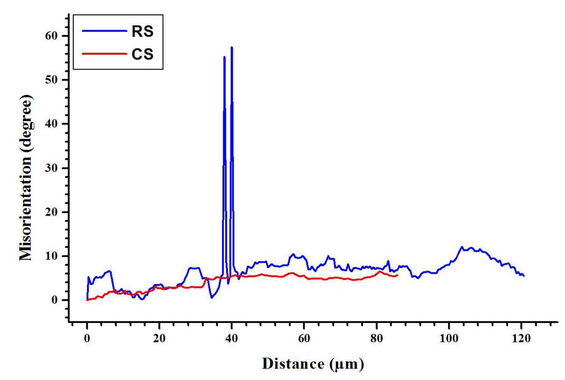

Figure 6. Misorientation distribution profile corresponding to [111] oriented grains highlighted by white lines in Figures. 3c and 4c

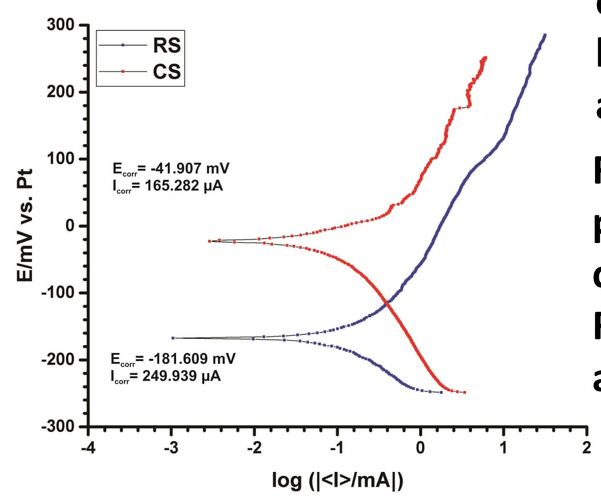

Figure 7. Potentiodynamic polarization curves comparing corrosion behaviour between RS and CS in the eutectic salt at 450˚C

References

Bauer, T., N. Pfleger, D. Laing, W.-D. Steinmann, M. Eck and S. Kaesche (2013). 20 - High-Temperature Molten Salts for Solar Power Application. Molten Salts Chemistry. F. L. Groult. Oxford, Elsevier: 415-438.

Boehlert, C. J., D. S. Dickmann and N. N. C. Eisinger (2006). "The effect of sheet processing on the microstructure, tensile, and creep behavior of INCONEL alloy 718." Metallurgical and Materials Transactions A 37(1): 27-40.

Fournier, L., D. Delafosse and T. Magnin (2001). "Oxidation induced intergranular cracking and Portevin–Le Chatelier effect in nickel base superalloy 718." Materials Science and Engineering: A 316(1-2): 166-173.

Acknowledgements

This work is funded by the Australian Solar Thermal Research Initiative (ASTRI), which is supported by the Australian Government via the Australian Renewable Energy Agency (ARENA). The data reported in this paper were obtained at the Central Analytical Research Facility (CARF) operated by the Institute for Future Environments at Queensland University of Technology (QUT). Access to CARF was supported by generous funding from the Science and Engineering Faculty (QUT).